

## **COMPARISON OF OXIDATION POWER SENSOR WITH COUPLED MULTIELECTRODE ARRAY SENSOR FOR MONITORING GENERAL CORROSION**

Xiaodong Sun and Lietai Yang  
Corr Instruments, LLC  
San Antonio, TX

### **ABSTRACT**

A simple oxidation power sensor (OPS) that has only a single electrode was proposed for the measurements of the bounding corrosion rates of actual equipment components. The OPS electrode is made from a non-consumable noble metal and does not need frequent changes or maintenance. The electrode of the OPS is placed near and electrically coupled to the system components to be measured. A modified OPS that has multiple electrodes and provides a correction factor for the estimation of the corrosion rate from the bounding corrosion rate was also proposed.

Verification tests were conducted in parallel with a coupled multielectrode array sensor for carbon steel in selected solutions. It was found that there was a good agreement between the trends of the bounding corrosion rates from the simple OPS and the localized corrosion rates from the CMAS probe. There was also an excellent agreement between the corrosion rate from the modified OPS in simulated seawater and the reported general corrosion rate obtained in long term-immersion tests in actual seawater.

**Keywords:** corrosion sensor, corrosion monitoring, oxidation power sensor, oxidation capacity sensor, cathodic capacity sensor, non-destructive sensor, multielectrode sensor, online corrosion sensor, real-time corrosion sensor, coupled electrodes, coupled multielectrode, multiple electrodes, galvanic sensor.

### **INTRODUCTION**

Low-cost sensors for quantitative corrosion monitoring for engineering structures and process equipments are highly desirable tools for corrosion control. These structures and equipments include pipelines (both external and internal), concrete re-enforcements (re-bars), airplanes, vehicles, bridge structures (including suspension cables), and equipments used in oil and gas fields, and chemical or power plants. Many of the structures and equipments are coated with protective coatings and corrosion only takes place in isolated areas on coated surfaces. An effective monitoring program requires the deployment of a massive number of sensors installed in critical areas or sensors that provide extensive coverage for large equipment. Another desired requirement for the sensors is the ability of providing the corrosion rate information for the actual equipment. Existing probes such as electrical resistance (ER)

#### Copyright

©2009 by NACE International. Requests for permission to publish this manuscript in any form, in part or in whole must be in writing to NACE International, Copyright Division, 1440 South creek Drive, Houston, Texas 777084. The material presented and the views expressed in this paper are solely those of the author(s) and are not necessarily endorsed by the Association. Printed in the U.S.A.

probes for general corrosion and coupled multielectrode array sensor (CMAS) probes for localized corrosion are excellent tools for real time corrosion monitoring. But the CMAS probes are generally expensive because of the multichannel requirements and the measurements for low-level currents<sup>1,2</sup> and the ER probe has limited life and requires frequent changes of the sensing element.<sup>3</sup> In addition, the ER probes measure the electrical resistance changes due to the cumulative corrosion-induced metal thinning and thus have slow responses. Linear polarization resistance (LPR) method is another widely used online method and gives near instant quantitative corrosion rate for general corrosion.<sup>4</sup> This method is, however, derived on the assumption that the corrosion processes are controlled by activation processes. In cases where the corrosion processes are controlled by both activation and diffusion, the LPR method may not be applicable.

In most cases, all of the above three methods measure the corrosion rate of the probe sensing element that is made with a metal that closely matches the system component to be monitored, in chemical composition and metallurgical conditions. The corrosion rates obtained from these probes are not the corrosion rate of the actual system components.

Non-destructive evaluation methods, such as ultrasonic method<sup>5</sup> and the electrical resistance field method (or called field signature method by some suppliers)<sup>6</sup> have been used to directly monitor the rate of corrosion that takes place on the actual pipe or equipment walls. Because the ultrasonic probe has a relatively low resolution ( $>10\ \mu\text{m}$ ), and the electrical resistance field method is based on the ER probe principle, both of these two methods are slow and neither can provide the information that can be used to aid for the day-to-day operations in a plant or a field. In addition, these two methods generally require the use of high-cost instruments.

This paper describes a single electrode probe that measures the local oxidation power or cathodic capacity and provides a bounding corrosion rate for actual system components in processes or in the fields. The electrode of this probe is a non-corroding metal and it does not require replacement. Thus, it is simple and low-cost and can be employed in large numbers in critical areas for corrosion surveillance. The metals or components that may be monitored with this probe include those under degraded coatings, buried in soils or embed in concrete. When additional electrodes are incorporated into the single-electrode probe, the bounding corrosion rate may be calibrated and used to estimate the actual corrosion rate taking place on the surface of the actual metal components based on the currents measured from the additional electrodes.

## PRINCIPLE

### Single Electrode Oxidation Power Sensor for Measurement of Bounding Corrosion Rate

Figure 1 shows the schematic diagram of a single-electrode oxidation power sensor (OPS) for corrosion. The working electrode is a noble metal electrode or non-corroding electrode. It can be of any electrode that is significantly more corrosion-resistant and more catalytically active for the cathodic reactions than the corroding metal. The noble metal electrode is controlled at the same potential as the corroding metal (the metal equipment or structure to be monitored) by coupling the noble electrode to the corroding metal through a zero-voltage ammeter (an ammeter that does not introduce a voltage when inserted into the circuit). The cathodic current density from this noble metal electrode may be used as the bounding corrosion current density for the corroding metal. Figure 2 shows the working principle of the bounding oxidation power sensor. The two thin curves represent the reduction current density on a corroding metal electrode caused by the oxidizing species in the electrolyte and the corrosion current density of the corroding metal itself, respectively. When the two curves meet, the potential is equal to the corrosion potential of the corroding metal ( $E_{\text{corr}}$ ), and the current density is

---

\* Strictly speaking, the corroding metal is another electrode and this system is a two-electrode system. Because the probe itself only contains one electrode, it is called a single-electrode sensor or probe in this paper.

equal to the corrosion current density ( $i_{corr}$ ). Similarly, the two thick curves represent the reduction current density caused by the oxidizing species in the electrolyte and the oxidation current density on the noble metal electrode, respectively. When the two thick curves meet, the potential is the open-circuit potential of the noble metal electrode ( $E_{oc,nbl}$ ). Because the noble metal is selected such that it is more catalytically active for the reduction reactions of the oxidizing species in the electrolyte, the thick cathodic curve is always on the right of the thin cathodic curve. Therefore, the cathodic current density on the noble metal electrode always bounds the cathodic current density on the corroding metal electrode. In addition, the externally measured reduction current density from the noble metal electrode equals the reduction current density caused by the oxidizing species in the electrolyte because the noble metal electrode does not corrode at the corrosion potential of the corroding metal (no oxidation current effect, assuming that the solution does not contain any other reducing species that can be oxidized on the noble metal electrode at the corrosion potential). For uniform corrosion, the corrosion current density ( $i_{corr}$ ) is equal to the reduction current density on the corroding metal electrode. Therefore,  $i_{corr}$  is less or equal to the reduction current density measured on the noble metal electrode ( $i_{bound}$ ).

It should be mentioned that the  $i_{bound}$  value obtained from the noble metal electrode may not be used to bound the localized corrosion current density because localized corrosion is usually supported by the cathodic current not only from the corroding section, but also from the other sections, especially the non-corroding sections (i.e., localized corrosion involves small anodes supported by large cathodes). The  $i_{bound}$  only bounds the corrosion current density averaged over a given surface area of the corroding metal, or the average corrosion current density, which corresponds to uniform corrosion rate.

Because the bounding reduction current density that can take place on a corroding metal corresponds to the bounding oxidation power of an electrolyte for the dissolution of the corroding metal, this method is called oxidation power sensor (OPS) (or oxidation capacity sensor). It can also be called a bounding cathodic current capacity sensor. Because the sensing electrode in Figure 1 is galvanically coupled to the corroding metal, this type of sensor may also be called galvanic oxidation power sensor. It should be mentioned, however, this type of sensor is fundamentally different from the commonly used galvanic sensors because in a galvanic sensor, the primary sensing electrode is usually a corrodible metal and the second electrode is a noble electrode which is used to raise the potential of the corrodible metal electrode from its corrosion potential to a higher potential. The galvanic sensor operates at raised potentials and measures only the qualitative corrosivity.<sup>7</sup> Contrary to the usual galvanic sensors, in an OPS, the primary sensing electrode is the noble metal and the potential of the noble metal is maintained at the corrosion potential of the corroding metal. In addition the OPS is meant to measure the quantitative bounding corrosion rate.

### Multiple Electrode Oxidation Power Sensor for Measurement of Corrosion Rate

Figure 3 shows the principle for a multiple electrode OPS that may be used for the measurement of corrosion rate. In Figure 3, the thick dashed curve is obtained by scaling the reduction current density curve on the noble metal ( $i_{nbl}$ ) by a constant factor ( $c$ ) so that the thick dashed curve (calibrated reduction curve or corrected reduction curve) meets the actually measured reduction curve (think dashed curve) on the corroding metal electrode ( $i_{msrd}$ ) at low potentials:

$$i_{msrd} = c \cdot i_{nbl} \quad (1)$$

The average corrosion rate ( $i_{corr}$ ), which is usually the uniform corrosion rate, may be estimated by the corrected current density from the oxidation power sensor ( $i'$ ):

$$i' = c \cdot i_{bound} \quad (2)$$

Figure 4 shows the schematic diagram of a multiple electrode OPS probe for measuring corrosion rate. In addition to the noble metal electrode as shown in Figure 2 (first noble electrode in Figure 4), there are another noble electrode (second noble electrode), a separate corroding metal electrode (second corroding metal electrode), and a sacrificial anode. The first zero-voltage ammeter ( $ZVA_1$ ) measures the current from the first noble electrode and provides the bounding corrosion current density ( $i_{bound}$ ) as discussed above. The second noble electrode and the second corroding metal electrode are both coupled to the sacrificial anode so that the two electrodes are at such a potential that the reduction curve actually measured on the corroding metal electrode (the thin dashed curve in Figure 3) meet the curve for the reduction of the oxidizing species on the corroding metal electrode (the thin solid reduction curve). Under this condition, the current densities from  $ZVA_3$  and  $ZVA_2$  as shown in Figure 4 are the values of  $i_{msrd}$  and  $i_{nbl}$  in Figure 3, respectively:

$$i_{msrd} = I(ZVA_3)$$

$$i_{nbl} = I(ZVA_2)$$

Where  $i(ZVA_2)$  is the current density measured from  $ZVA_2$  and  $i(ZVA_3)$  is the current density measured from  $ZVA_3$ . Therefore, the value of  $c$  can be calculated according Eq. (1) and the corrosion current ( $i_{corr}$ ) can be estimated by Eq. (2):

$$i_{corr} \approx i_{bound} \cdot i(ZVA_3)/i(ZVA_2) \quad (3)$$

## EXPERIMENTS

### Single Electrode Approach

A 20-electrode nanoCorr<sup>\*</sup> coupled multielectrode array sensor (CMAS) corrosion monitor was used to verify the performance of the single electrode oxidation power sensor against a CMAS probe. Figure 5 shows the connections between the CMAS monitor and the CMAS probe (with carbon steel electrodes) and the oxidation power sensor. The CMAS monitor acted as a multichannel zero-voltage ammeter that coupled the multiple carbon steel electrodes of the CMAS probe to a coupling joint and measures the individual currents. The coupling joint of the CMAS monitor is then connected to the noble electrode of the oxidation power sensor. The sum of the currents measured by the multichannel ZVAs in the CMAS monitor for the currents from the multiple electrodes equals the net current to or from the noble electrode. A reference electrode [saturated Silver-Silver Chloride electrode (SSE)--not shown in Figure 5] was also connected to the CMAS monitor that can measure the corrosion potential of the CMAS probe (or the potential of the coupling joint). Therefore the CMAS probe in Figure 5 served for dual purposes. One purpose was to provide the corrosion rate for comparison with the oxidation power sensor, and the other purpose was that the collection of the multiple carbon steel electrodes in the CMAS probe acted as the corroding metal as shown in Figure 1.

The CMAS probe used in the experiment was a commercial combination CMAS probe that contains 14 Type 1008 carbon steel (UNS G10080) wire (0.89 mm in diameter) electrodes and two platinum wire (1 mm in diameter) electrodes, all flush-mounted in a polytetrafluoroethylene (PTFE) insulation (Figure 6). The 14 carbon steel electrodes were connected to the multichannel connector of the CMAS monitor and used as the carbon steel CMAS probe (Figure 5).

In the first experiment, one of the platinum electrodes in the combination CMAS probe was connected to the coupling joint of the CMAS monitor and used as the noble electrode of the oxidation power sensor (Figure 5). In the second experiment, a Type 110 copper (UNS C11000) wire (1 mm in diameter) flush mounted in an epoxy insulation was connected to the coupling joint of the CMAS monitor (Figure 5) and used as the noble electrode for the oxidation power sensor.

---

\* Trademark of Corr Instruments, LLC, San Antonio, Texas, USA.

All data were saved to the on-board memory of the CMAS monitor and also transmitted to the wireless Ethernet and RS-232 interfaces of the CMAS field monitor on real time basis.

A notebook computer with the CMAS corrosion monitor software that supports multichannel measurements and real time data acquisition and local or remote interfacing with the CMAS monitor via the RS-232 or Ethernet interface both locally or remotely was used to gather the data from the CMAS monitor.

### **Multiple Electrodes Approach**

A 40-channel zero-voltage ammeter (ZVA) by the same company that manufactured the CMAS corrosion monitor was used to verify the performance of the multiple electrode oxidation power sensor against a CMAS probe. Figure 7 shows the connections between the multichannel zero-voltage ammeter and the CMAS probe and the oxidation power sensor. The multichannel ZVA has four independent 10-channel banks and four corresponding independent coupling joints. The first two banks (Banks 1 and 2) of channels (for maximum of 20 channels) were used as the first group of ZVA channels for the CMAS probe, and coupled the electrodes of the CMAS probe to a coupling joint (combined Bank 1 and 2 coupling joint) and measured the individual currents. The Banks 1 and 2 coupling joints were combined and then connected to the first noble electrode of the oxidation power sensor. The sum of the currents measured by the first groups of ZVA channels for the currents from the multiple electrodes of the CMAS probe equals the net current to or from the first noble electrode. The third bank of the ZVA channels were used as the second group of the ZVA channels that coupled the second noble electrode and the second corroding metal electrode to the sacrificial anode via Bank 3 coupling joint.

A SSE reference electrode (not shown in Figure 7) was also connected to the ZVA that can measure the corrosion potentials of the CMAS probe (or the potential of the Bank 1 and 2 coupling joints) and the potential of the Bank 3 coupling joint (the coupling potential of the sacrificial anode, the second noble electrode and the second corroding metal electrode). Same as in Figure 5, the CMAS probe in Figure 7 also served for dual purposes. One purpose was to provide the corrosion rate for comparison with the oxidation power sensor, and the other purpose was that the multiple electrodes in the CMAS probe acted as the corroding metal as shown in Figure 4.

The CMAS probe was the same probe as shown in Figure 6. The first 13 carbon steel electrodes were connected to the first multichannel connector (combination of Bank 1 and 2) of the ZVA (Figure 7) and used as the carbon steel CMAS probe. The 14<sup>th</sup> carbon steel electrode was connected to the 2<sup>nd</sup> channel of the second group of ZVA channels and used as the 2<sup>nd</sup> corroding metal electrode. One of the platinum electrodes was connected to Banks 1 and 2 coupling joints and used as the oxidation power sensor's 1<sup>st</sup> noble electrode. The other platinum electrode of the combination CMAS probe (Figure 6) was connected to the 1<sup>st</sup> channel of the second group of ZVA channels and used as the 2<sup>nd</sup> noble electrode. A bare pure aluminum wire (1 mm in diameter and approximately 7 cm in length immersed in the electrolyte) was connected to the coupling joint of the second group of ZVA channels (Bank 3 coupling joint) and used as the sacrificial anode as shown in Figure 4.

Same as the CMAS monitor described previously, all data were saved to the on-board memory of the multichannel ZVA and also transmitted to the wireless Ethernet and RS-232 interfaces of the ZVA on real time basis.

A notebook computer with the software that supports the multichannel measurements and real time data acquisition was used to gather the data from the multichannel ZVA via the wireless Ethernet interface.

## RESULTS AND DISCUSSIONS

### Single Electrode Approach for Bounding Corrosion Rate

Figure 8 shows the typical bounding average corrosion rates for carbon steel in bottled drinking water (Ozarka natural spring water) obtained with the OPS formed by a platinum and a copper noble electrodes, respectively. The corrosion rates from the CMAS probe with 14 carbon steel sensing electrodes are also shown in Figure 8. The bounding corrosion rates for carbon steel measured with both the copper OPS and platinum OPS probes varied from 0.4 to 0.6 mm/yr. The localized corrosion rate from the CMAS probe varied from 0.5 to 0.9 mm/yr and the average corrosion rate from the CMAS probe was about 0.22 mm/yr. If the average corrosion rate from a carbon steel CMAS probe can be used to estimate the general corrosion rate of carbon steel in the drinking water<sup>8</sup>, the average corrosion rate from the CMAS probe should be bounded by the bounding corrosion rate obtained from the OPS, which is consistent with the results shown in Figure 8. The corrosion potential was about -0.6 V (SSE) after the CMAS probe was decoupled from the platinum electrode, but increased slightly when it was coupled to the Cu electrode, suggesting that the Cu electrode surface area should be further reduced to not have any effect on the corrosion potential of the corroding metal.

Figure 9 shows the comparison of the bounding corrosion rates obtained with the copper and platinum OPS probes and the localized corrosion rates and the corrosion potential obtained with the CMAS probe for carbon steel. In general, the higher the localized corrosion rates from the CMAS probe were, the higher the bounding corrosion rates measured with the OPS probes were. Figure 9 also shows that, in cases with less corrosive environments (seawater, tap water and bottled drinking water), the bounding corrosion rate from the OPS probe was lower (did not bound) than the localized corrosion rate from the CMAS probe. This is because the OPS probe measures the maximum possible corrosion current assuming the corrosion is taking place uniformly on the entire surface of the corroding metal, while localized corrosion is usually supported by the cathodic current not only from the corroding section, but also from the other sections, especially the non-corroding sections (see the Principle Section). It should be noted that the average corrosion rates from the CMAS probe were not presented in Figure 9 because the average corrosion rate is more subject to the internal current effect in 0.4wt%HCl solution which causes dominantly uniform corrosion for carbon steel and cannot be effectively detected by the CMAS probe.<sup>9,10</sup>

The corrosion potentials were approximately -0.6 V(SSE) in seawater, tap water and bottled drinking water, and increased slightly in the 0.4wt% HCl and 2wt%HCl + 1.6wt%FeCl<sub>3</sub> solutions due to the presence of Fe<sup>3+</sup> and higher concentrations of H<sup>+</sup>.

### Multiple Electrode Approach for Corrosion Rate

Figure 10 shows the real-time localized corrosion rate from a carbon steel CMAS probe and the corrected (calibrated) corrosion rate (corresponds to  $i'$  in Eq. 2 or  $i_{\text{corr}}$  in Eq. 3) and other related parameters obtained using the setup as shown in Figure 7 in different solutions. The other parameters include the bounding corrosion rate from the first Pt electrode (corresponds to  $i_{\text{bound}}$  in Eq. 3), the rate from the second Pt electrode (corresponds to  $i(\text{ZVA}_2)$  in Eq. 3) and rate from the second corroding metal electrode (corresponds to  $i(\text{ZVA}_3)$  in Eq. 3). The potentials of the two corroding metals are also shown in the diagram. The difference between the two potentials was between 90 and 130 mV so that the anodic current (the internal current) on the second corroding metal electrode is expected to be near zero and the measured current density from the second corroding metal should be close to the cathodic current density on the second corroding metal (The thin solid curve meets the thin dashed curve as shown in Figure 3). It should be mentioned that the potentials shown in Figure 10 are not required during corrosion monitoring as long as it has been demonstrated/verified that the sacrificial anode had the ability to maintain the appropriate potential (not too high which cannot eliminate the anodic current or internal current effect; and not too low which causes other oxidizing species, that are normally stable at the corrosion potential, to react and to contribute to the reduction current density).

Figure 11 shows the comparison for the time-averaged carbon steel corrosion rates derived from Figure 10 in the three different environments. The time-averaged and corrected corrosion rate (corresponds to  $i'$  in Eq. 2 or  $i_{corr}$  in Eq. 3) for carbon steel are 3, 15, and 0.3 mm/yr in 0.4% HCl solution, 2% HCl + 1.6% FeCl<sub>3</sub> solution, and seawater, respectively. The value obtained in seawater (0.3 mm/yr) is in excellent agreement with the general corrosion rate for carbon steel obtained from a 1-year immersion tests in Panama Canal seawater (0.228 mm/yr).<sup>11</sup>

## CONCLUSIONS

A low-cost and simple single electrode sensor, called oxidation power sensor (OPS), was proposed for the measurements of the bounding corrosion rates of actual metal components of process or field equipment. The OPS has a non-consumable noble metal electrode as the sensing electrode and there is no need to change or replace the sensing electrode during the measurements. In addition, the OPS is a non-destructive sensor and causes no disturbance to the actual system components whose corrosion rates are to be measured. The OPS may be used to measure or detect corrosion for metals in liquid or film electrolytes, under coatings and in soil.

A modified OPS that has multiple electrodes and provides a correction factor for the estimation of the corrosion rate from the bounding corrosion rate was also proposed.

Verification testes were conducted for carbon steel in several solutions and the performance of the OPS probe was compared with that of a coupled multielectrode array sensor (CMAS) probe. In general, the trends of the bounding corrosion rates from the simple OPS and the localized corrosion rates from the CMAS probe agreed well in the different solutions. There was also an excellent agreement between the corrected corrosion rate from the multiple electrode OPS for carbon steel in simulated seawater and the general corrosion rate reported in the literature.

## REFERENCES

1. L. Yang, "Multielectrode Systems," in "Corrosion Monitoring Techniques," L. Yang, ed., Woodhead Publishing, Success, UK, (2008), Chapter 8.
2. L. Yang, N. Sridhar, O. Pensado, and D. Dunn, "An In-Situ Galvanically Coupled Multi-Electrode Array Sensor for Localized Corrosion," *Corrosion*, 58 (2002), p. 1004.
3. C.S. Brossia, "Electrical Resistance Techniques," in "Corrosion Monitoring Techniques," L. Yang, ed., Woodhead Publishing, Success, UK, (2008), Chapter 11.
4. S. Papavinasam, "Electrochemical Techniques for Corrosion Monitoring," in "Corrosion Monitoring Techniques," L. Yang, ed., Woodhead Publishing, Success, UK (2008), Chapter 3.
5. G. Light, "Nondestructive evaluation Technologies for Monitoring Corrosion," in "Corrosion Monitoring Techniques," L. Yang, ed., Woodhead Publishing, Success, UK (2008), Chapter 12.
6. N.N. Bich, "Corrosion Monitoring Using the Field Signature Method Inspection Tool," in "Corrosion Monitoring Techniques," L. Yang, ed., Woodhead Publishing, Success, UK (2008), Chapter 28.
7. R.D. Klassen and P.R. Roberge, "Zero Resistance Ammetry and Galvanic Sensors," in "Corrosion Monitoring Techniques," L. Yang, ed., Woodhead Publishing, Success, UK (2008), Chapter 5.
8. X. Sun and L. Yang, "Real-Time Monitoring of Localized and General Corrosion Rates in Simulated Marine Environments Using Coupled Multielectrode Array Sensors," *CORROSION/2006*, paper no. 06284, Houston, TX: NACE, 2006.
9. L. Yang and K.T. Chiang, "Electrochemical Behavior and Internal Current of the Most Anodic Electrode in a Coupled Multielectrode Array Sensor," *Proceedings of the 17<sup>th</sup> international Corrosion Congress*, 2008.
10. L. Yang and K.T. Chiang, P K. Shukla, and N. Shiratori, "Internal Current Effects on Localized Corrosion Rate Measurements Using Coupled Multielectrode Array Sensors," submitted to *CORROSION/2009*, paper no. 09446, Houston, TX: NACE, 2009.
11. S.R. Southwell and A.L. Alexander, "Corrosion of Metals in Tropical Water-Structural Ferrous Metals", *Materials Protection*, Vol 9, No. 1, 1970, p.14.

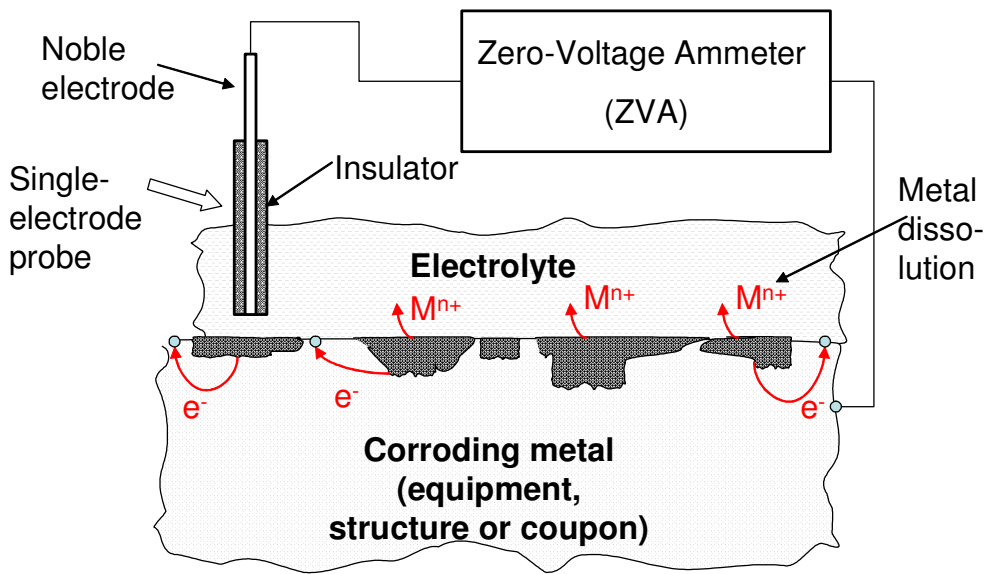


**FIGURE 1.** Schematic diagram of a single electrode oxidation power sensor for corrosion. Note: Patent pending.

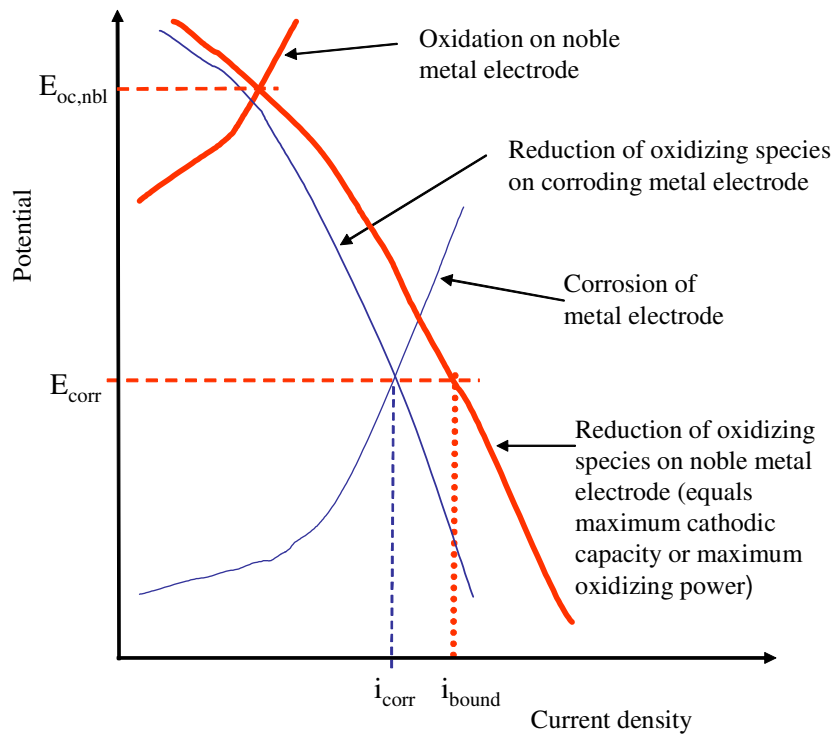


**FIGURE 2.** Working principle of a single electrode oxidation power sensor for measuring bounding corrosion rate.

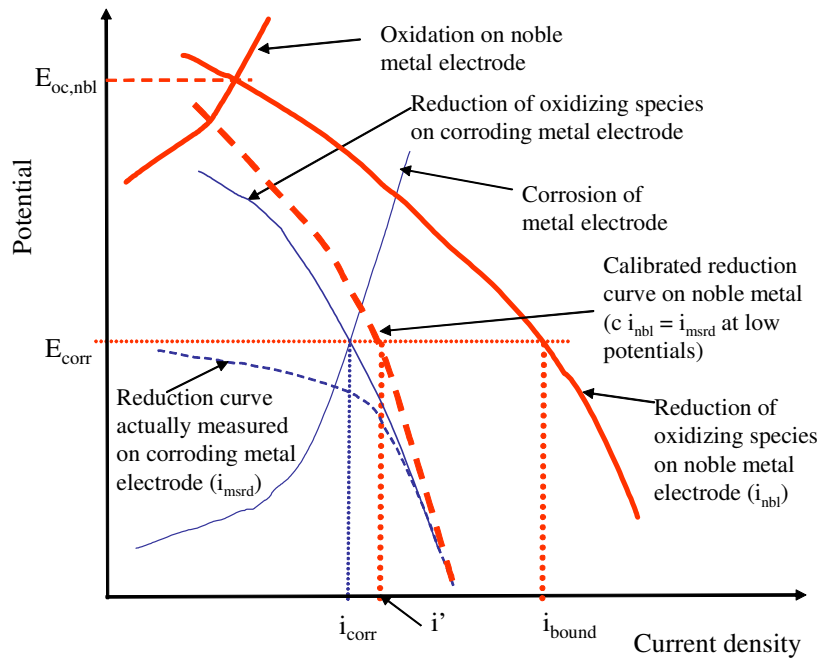


**FIGURE 3.** Working principle for a multiple electrodes oxidation power sensor for measuring corrosion rate.

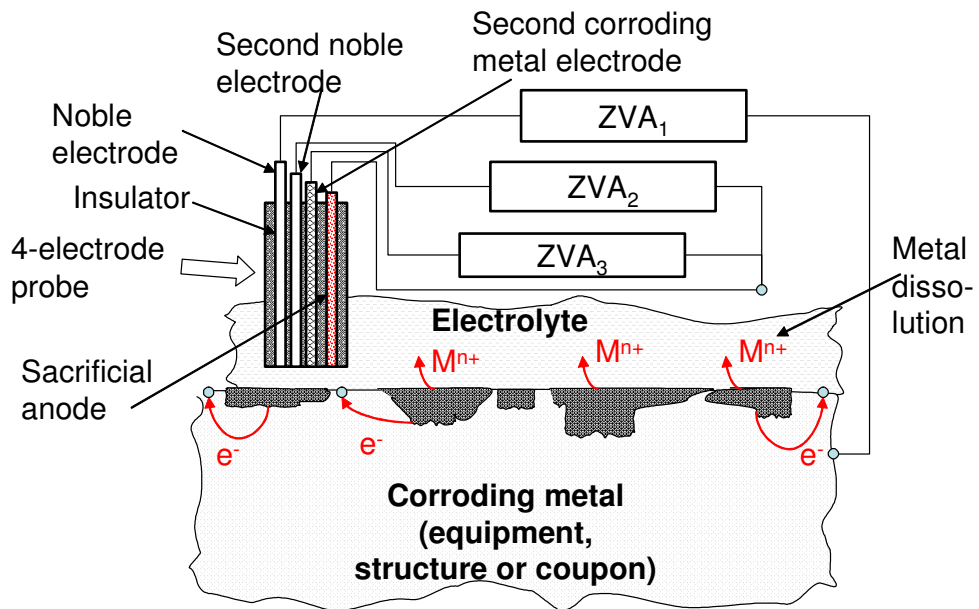


**FIGURE 4.** Schematic diagram of a multiple electrodes oxidation power sensor for measuring corrosion rate. Note: Patent pending.

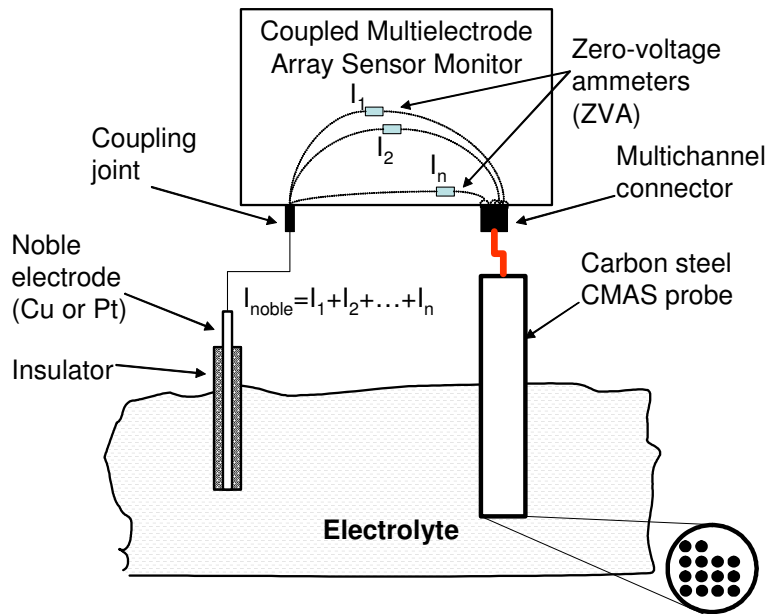


**FIGURE 5.** Experimental setup for using a CMAS probe to verify the performance of a single electrode oxidation power sensor. Note: The coupling joint of the CMAS probe was connected to the noble metal through the ZVAs to use the carbon steel electrodes of the CMAS probe as the corroding metal as shown in Figure 1.

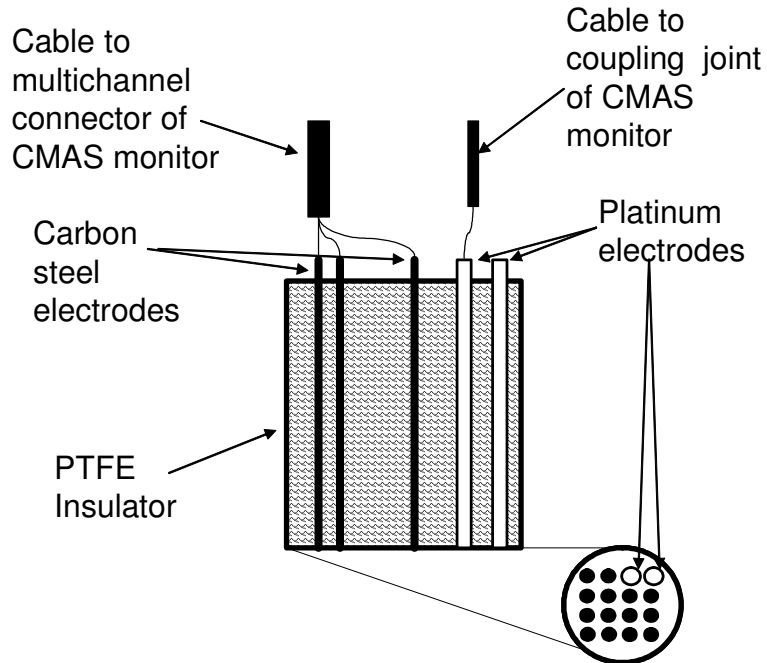


**FIGURE 6.** Schematic diagram of a commercial combination coupled multielectrode probe used in the experiment. Note: The 14 carbon steel electrodes were for the CMAS probe and the two platinum electrodes were for the noble electrodes.

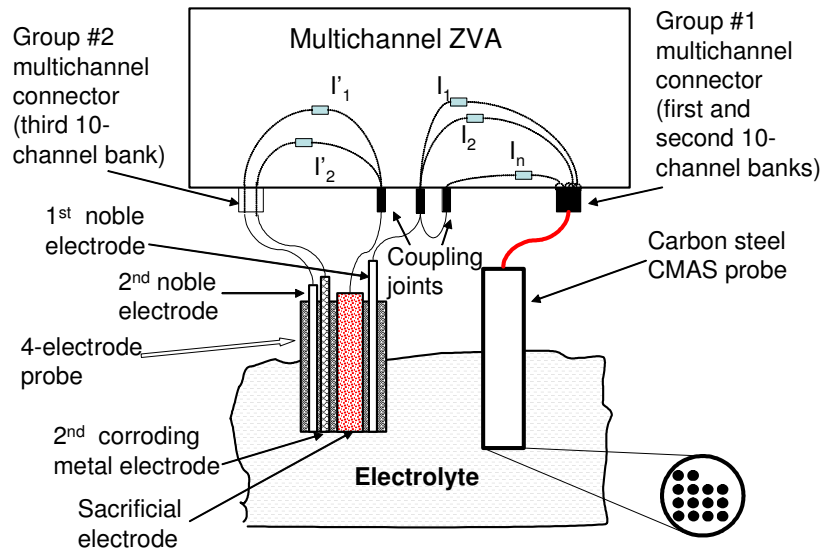


**FIGURE 7.** Experimental setup for using a CMAS probe to verify the performance of a multiple electrode oxidation power sensor. Note: The multichannel ZVA has four independent 10-channel banks and four corresponding independent coupling joints. The first two banks (Banks 1 and 2) were used for the CMAS probe and the third bank was used for the 2nd noble and 2nd corroding metal electrodes.

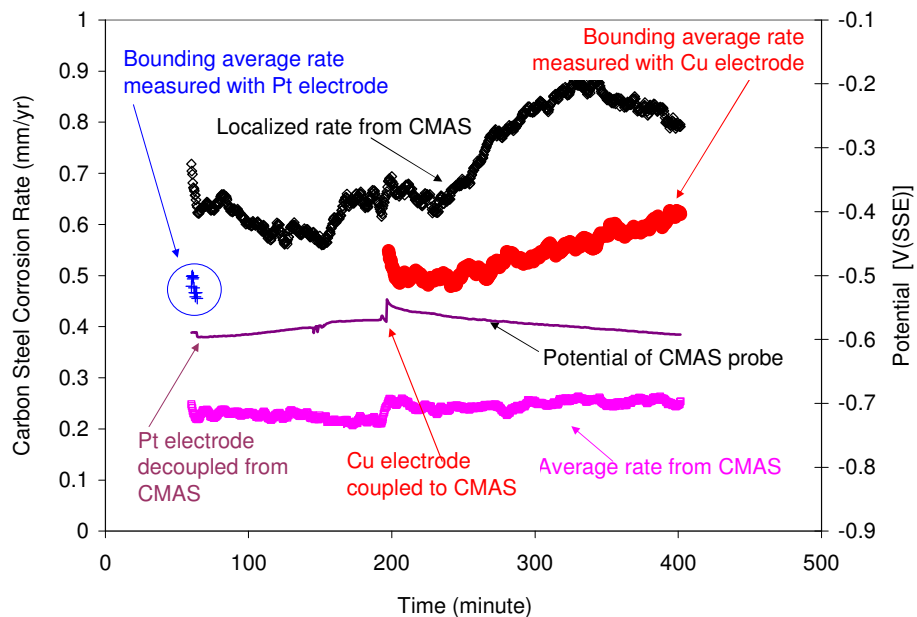


**FIGURE 8.** Typical bounding corrosion rate for carbon steel in drinking water obtained with the oxidation power sensors formed with platinum and copper noble electrodes, and corrosion rates and the corrosion potential obtained from a CMAS probe.

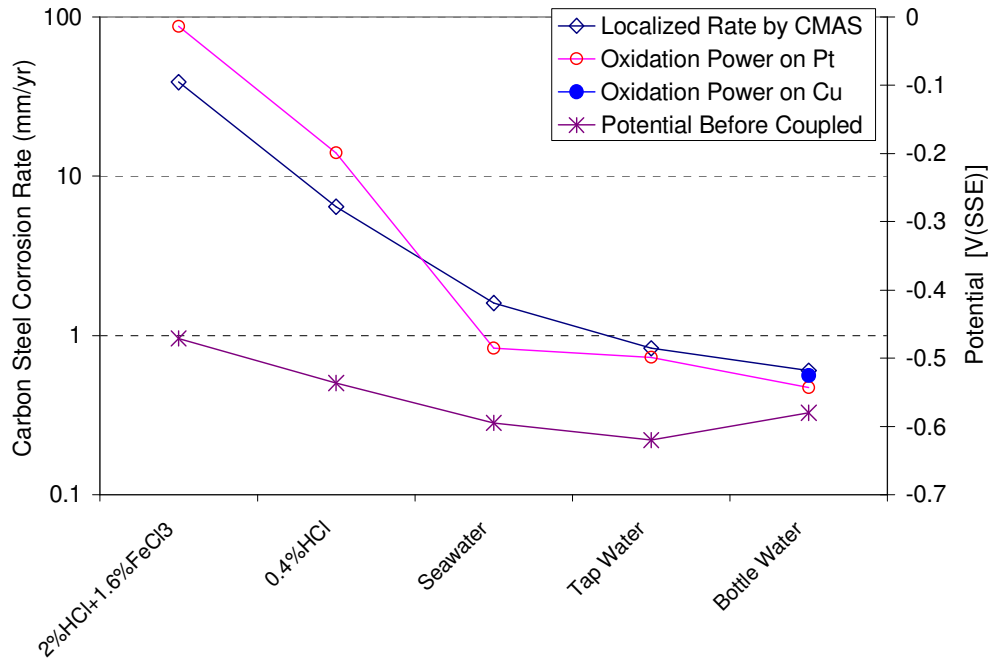


**FIGURE 9.** Comparison of the oxidation powers (bounding corrosion rates) obtained with the platinum and copper OPS probes, and the localized corrosion rate and the corrosion potential obtained from the CMAS probe for carbon steel.

Note: Corrosion potential was measured at the coupling joint of the CMAS monitor before it was connected to the noble electrodes.

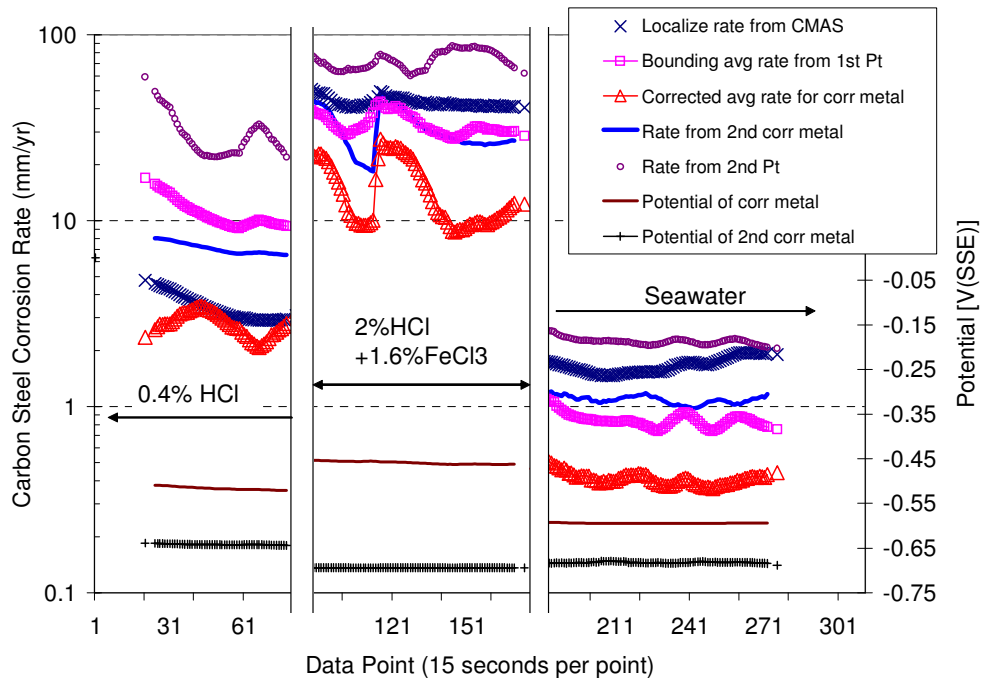


**FIGURE 10.** Typical corrected average corrosion rate and related parameters obtained with a multiple electrode OPS probe in different solutions and localized corrosion rate from a CMAS probe.

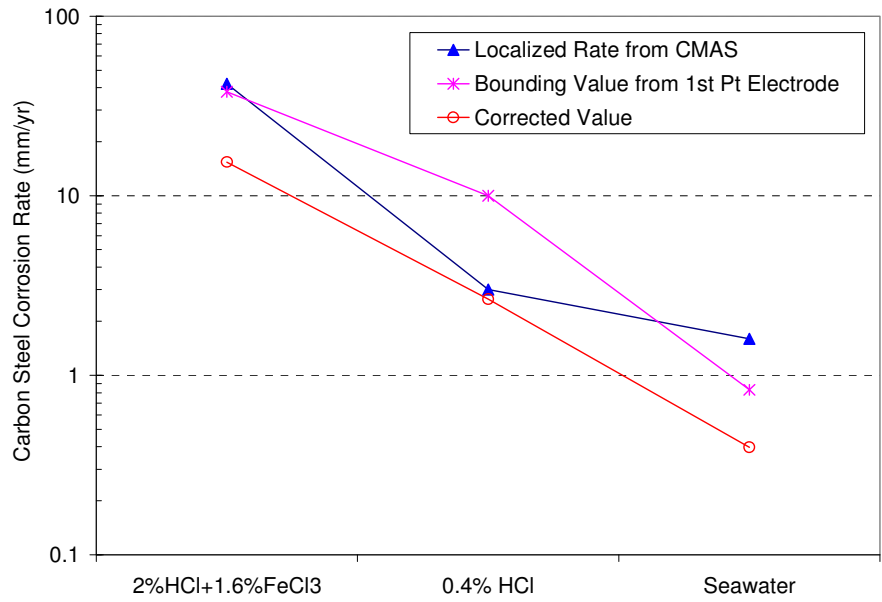


**FIGURE 11.** Comparison of the corrected corrosion rates and bounding corrosion rates from a multiple electrode OPS probe, and the localized corrosion rate from a CMAS probe for carbon steel.